RESEARCH ARTICLE

Pre-existing fractures and eruptive vent openings during the 2021 Fagradalsfjall eruption, Iceland

Ásta Rut Hjartardóttir[1] · Tobias Dürig[1] · Michelle Parks[2] · Vincent Drouin[2] · Vigfús Eyjólfsson[1] · Hannah Reynolds[1] · Páll Einarsson[1] · Esther Hlíðar Jensen[2] · Birgir Vilhelm Óskarsson[3] · Joaquín M. C. Belart[1,4] · Joël Ruch[5] · Nils B. Gies[3,6] · Gro B. M. Pedersen[1]

Abstract

The Fagradalsfjall eruption commenced on 19 March 2021 on a ~180-m-long eruptive fissure, following a 23-day dike intrusion. New eruptive fissures opened northeast of the initial eruption site on 5, 6–7, 10, and 13 April 2021. The northernmost eruption occurred on 5 April, approximately 1 km northeast of the initial fissure, with the other fissure openings between this and the initial eruptive vents. Still images from web cameras and time-lapse cameras are available for five of the fissure openings. These data show that the eruptions were preceded by steam emitted from cracks in the exact locations where the eruptions started. The time between the first steam observations and the visual appearance of glowing lava ranged between 15 s and 1.5 min during night observations and from 9 to 23 min during daytime observations. The difference in observation time is likely explained by the different lighting conditions. The eruptive vents are located where the north-easterly oriented dike intersected pre-existing north-south-oriented fractures, inferred to be strike-slip faults. These fractures could be identified on a high-resolution ICEYE interferogram as well as on pre-existing aerial photographs and digital elevation models. This interferogram spanned the first day of the eruption (19–20 March 2021). It not only displays deformation related to the pre-eruptive dike intrusion but also shows lineations in locations where eruptive vent openings occurred later in April 2021. These findings demonstrate how Interferometric Synthetic Aperture Radar Analysis (InSAR) can be used to forecast likely locations of subsequent eruptive vent openings, which is of great importance for hazard assessment and defining exclusion zones during fissure eruptions.

Keywords Eruption · Dike · Fractures · Vent openings · Fagradalsfjall · Strike-slip faults

✉ Ásta Rut Hjartardóttir
astahj@hi.is

1   Institute of Earth Sciences, University of Iceland, Reykjavík, Iceland

2   Icelandic Meteorological Office, Reykjavík, Iceland

3   Icelandic Institute of Natural History, Garðabær, Iceland

4   National Land Survey of Iceland, Akranes, Iceland

5   University of Geneva, Geneva, Switzerland

6   Institute of Geological Sciences, University of Bern, Bern, Switzerland

Introduction

Dike intrusions at divergent plate boundaries have only been instrumentally monitored a few times. These include the 1975–1984 Krafla rifting episode, the rifting episode in Asal-Ghoubbet in Djibouti in 1978, the 2005–2010 Dabbahu-Gabho rifting episode in Ethiopia, the 2007 dike intrusion in Tanzania, and the 2014 Bárðarbunga dike intrusion in Iceland (e.g., Björnsson et al. 1977; Abdallah et al. 1979; Wright et al. 2006; Biggs et al. 2009; Sigmundsson et al. 2015; Einarsson and Brandsdóttir 2021). In Hawaii, gravitational forces form the rift; the last rift intrusion and eruption occurred in 2018 (e.g., Neal et al. 2019).

These dike intrusions occur in rift zones. Eruptions in rift zones tend to take place on fissures. Eruptive fissures are generally oriented parallel to pre-existing open fissures and normal faults in the rift zones and perpendicular to the orientation

of the least principal stress (e.g., Nakamura 1977). The faults often form grabens, with the eruptive fissures in the middle or on the boundary of these grabens (e.g., Trippanera et al. 2015; Ruch et al. 2016). However, sometimes the eruptive fissures form without any visually observable graben formation.

Eruptions within the rift zones generally start through multiple fissure openings/vents producing a curtain of fire. As time progresses, most of the vents become inactive whereas some may continue for longer time periods. These changes in vent activity with time have been observed in different eruptions elsewhere, such as during the 2018 Kīlauea eruption in Hawai'i (Neal et al. 2019), and during the 2014 Holuhraun eruption in Iceland (Hjartardóttir et al. 2016). Vents tend to localize due to flow channeling, where the magma is focused on certain parts of the fracture with the largest aperture (Bruce and Huppert 1990; Gudmundsson 2020). How this focusing of eruptive activity happens can vary, as can the length of time from the beginning of steam emission from a fracture observed at the surface until the magma finally reaches the surface to form a new eruptive fissure.

This paper focuses on the opening of eruptive fissures in an unusual tectonic setting: an oblique rift where there is a high density of fractures categorized as normal faults, tensile fractures, or strike-slip faults. The 2021 Fagradalsfjall eruption in Reykjanes, Iceland, was thoroughly monitored by various methods, including webcams and aerial photography. Opening of new eruptive fissures could be observed, showing the relationship between pre-existing fractures, topography, and the location of the new eruptive fissures, as well as their behavior and the timescales involved.

Geological setting

The Reykjanes peninsula is located at the Mid-Atlantic plate boundary, where the Eurasian and North-American Plates are diverging at a rate of ~2 cm/year (e.g., Einarsson 1991; DeMets et al. 1994; Sella et al. 2002; Árnadóttir et al. 2009). Due to the oblique spreading, both normal and strike-slip faults, as well as tension fractures, can be found across the peninsula. The normal faults and tension fractures are concentrated in fissure swarms that cut obliquely across the plate boundary and extend into the tectonic plates on either side of it (Fig. 1). Eruptive fissures along the Reykjanes peninsula are usually found within fissure swarms (Klein et al. 1977; Jónsson
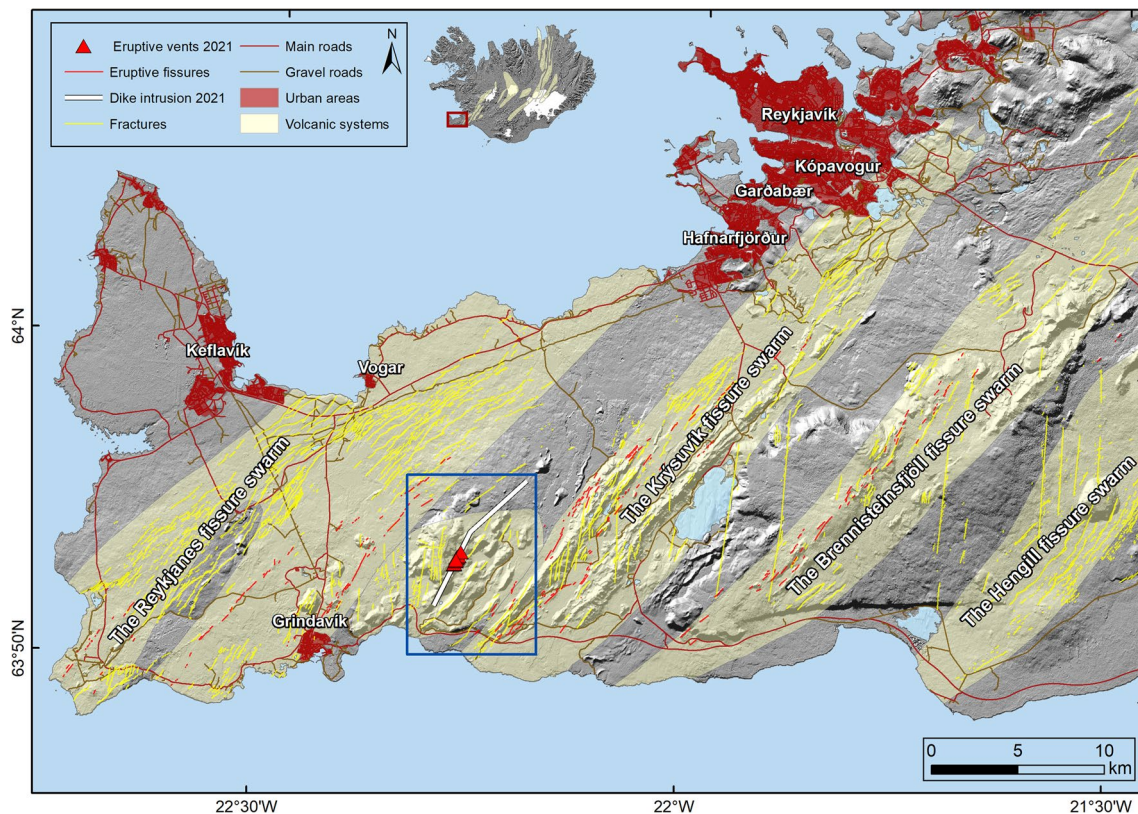

Fig. 1 Volcanic systems, fractures, and eruptive vents in the Reykjanes peninsula. The blue frame shows the location of the 2021 Fagradalsfjall eruption. The locations of fractures and eruptive fissures are from Clifton and Kattenhorn (2006). Information on vol-canic systems are from Sæmundsson and Sigurgeirsson (2013). Cartographic data are from the National Land Survey of Iceland. The location of the dike is from Sigmundsson et al. (2022). For a close-up of the eruption area, see Fig. 2

1978; Sæmundsson 1978; Guðmundsson 1987; Einarsson 1991; Hreinsdóttir et al. 2001; Clifton and Kattenhorn 2006; Einarsson 2008; Keiding et al. 2009; Villemin and Bergerat 2013). Studies of previous dike intrusions in Iceland suggest that such fissure swarms mainly become activated during dike intrusions (e.g., Sigurdsson 1980; Wright et al. 2012; Hjartardóttir et al. 2016; Ruch et al. 2016). The main fissure swarms on the Reykjanes peninsula are the Reykjanes fissure swarm, the Krýsuvík fissure swarm, and the Brennisteinsfjöll fissure swarm (Einarsson and Sæmundsson 1987). However, the 2021 Fagradalsfjall eruption occurred between the Reykjanes and Krýsuvík fissure swarms and not within them. The special characteristics of volcanism in the Fagradalsfjall area have led to its definition as a separate volcanic system, despite its lack of most of the typical features of such systems in Iceland (Sæmundsson et al. 2020; Einarsson et al. 2023).

The Reykjanes peninsula is largely covered by post-glacial lava flows and is highly volcanically active (Sæmundsson et al. 2010, 2020). Some of these postglacial lava flows extend into populated areas, such as the eastern part of the capital area

of Reykjavík (including the adjacent towns of Hafnarfjörður, Garðabær, and Kópavogur), and the towns of Grindavík and Vogar (Fig. 1). Studies of existing lava flows along the peninsula indicate that eruptions occur periodically, with multiple eruptions in different fissure swarms occurring intermittently for up to several hundred years, followed by a ~800–1000-year quiescence, when no eruptions occur (Sæmundsson et al. 2020). During the periods of quiescence, the seismicity is mostly caused by strike-slip faulting. The maximum compressive stress in the area alternates thus between being vertical and horizontal with a NE orientation, while the minimum compressive stress is consistently northwesterly oriented (Einarsson 1991).

The 2021 eruption at Fagradalsfjall followed a period of unrest that began in December 2019 with a modest earthquake swarm at the plate boundary in Fagradalsfjall and included several episodes of inflation and intrusions in at least three different areas of the plate boundary in Reykjanes (Geirsson et al. 2021; Halldórsson et al. 2022; Sigmundsson et al. 2022). The 2021 eruption was preceded by the propagation of a NE trending, 9-km-long dike intrusion that
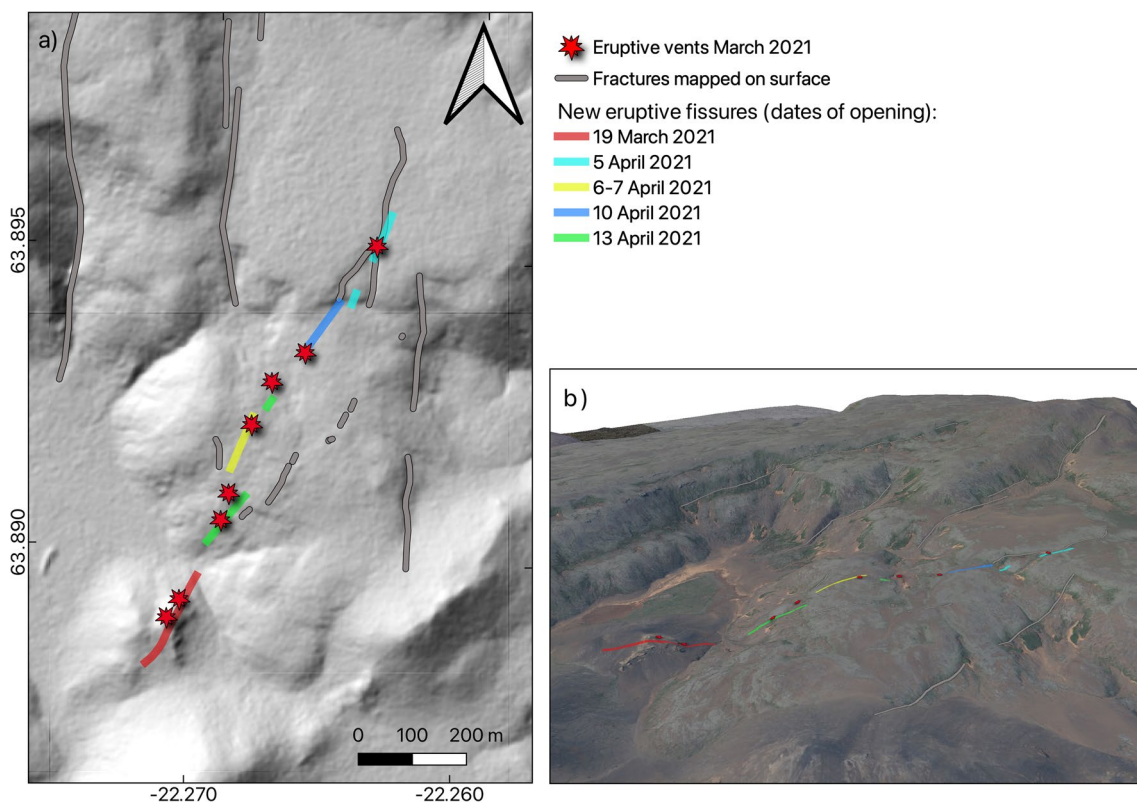

Fig. 2 (**a**) The location and time-evolution of the openings of the eruptive fissures during the 2021 Fagradalsfjall eruption. The fractures shown are the ones which were mapped from aerial photographs, digital elevation models, and during field work. (**b**) A 3D view of the eruptive fissures and the main eruptive vents, view towards the west. The image shows how the initial eruptive fissure opened in a topographical low whereas the subsequent fissure openings occurred higher up in the mountains. Note how the

northernmost eruptive fissure (farthest to the right) is located along a fracture (see also panel a). This fracture is clearly visible from the aerial photograph which was taken in July 2019, almost 2 years before the eruption started. The same fault is also visible on an aerial photograph taken in August 1985 by the National Land Survey of Iceland. The DEM is from the IslandsDEM of the National Land Survey of Iceland, the aerial photograph from Loftmyndir Corp. is draped on top of it

began on 24 February and was accompanied by an intense earthquake swarm along the plate boundary. The diking event culminated in an eruption on 19 March which lasted 6 months and produced a lava field of 4.8 km^2 area and a bulk volume of 0.15 km^3 (Pedersen et al. 2022).

Data and methods

New eruptive fissures and vents were mapped from aerial photographs taken during repeated surveillance flights over the unrest area in and close to Mt. Fagradalsfjall. These vertical aerial photographs were taken onboard the airplane of Garðaflug Corp., and onboard helicopters of the Icelandic Coast Guard (Pedersen et al. 2022). In a few cases, imagery from the web cameras of the Morgunblaðið newspaper and the Icelandic National Broadcasting Service (Ríkisútvarpið) was used to help locate the eruptive fissures. The vertical aerial photographs were processed photogrammetrically at the Icelandic Institute of Natural History and at the National Land Survey of Iceland, and georeferenced with an array of ground control points placed around the volcano (Pedersen et al. 2022). New fracture movements in the vicinity of the eruption were also detected on these images and were mapped in the field by Trimble ProXH GPS instruments. In addition, ICEYE Interferometric Synthetic Aperture Radar (InSAR) analysis was used to detect new fracture movements around the time when the first eruptive fissure opened. Fieldwork was done repeatedly during the eruption to survey and monitor new fracture movements. Pre-existing fractures in the area were mapped from aerial photographs from Loftmyndir Corp., and from digital elevation models (DEMs) from IslandsDEMs, which is based on ArcticDEMs (Porter et al. 2018; The National Land Survey of Iceland 2020). These fractures are displayed as lineaments on the images. The DEMs are particularly useful to detect vertical movements on faults.

The ICEYE interferogram used in this study spanned exactly 24 h, from 03:20:56 on 19 of March to 20 March. Bayesian inversions were run using the interferogram as the input to constrain parameters for the pre-eruptive dike and to derive an improved understanding of the magma plumbing system and structural controls, immediately prior to the onset of the eruption. These inversions were undertaken using GBIS software (Bagnardi and Hooper 2018) using rectangular dislocations (Okada 1985) to model both the dike and a single fault.

The timing and behavior of the opening of five of the new eruptive fissures and vents was found from stills on time-lapse cameras and web cameras. The two time-lapse cameras were operated by the Institute of Earth Sciences at the University of Iceland. They were located on a hill to the

south of the first (most western) fissure, from where they continuously photographed the landscape with a frame rate of 1 image per minute. The webcams were operated by the Morgunblaðið newspaper and the Icelandic National Broadcasting Service (Ríkisútvarpið) and provided the world with stunning live footage from the eruption site. These cameras were located to the south and east of the initial vent.

Results

The first eruptive fissure that opened on 19 March 2021 at approximately 20:30 was ~180 m long (Fig. 2). The eruption occurred on a small hill in a topographically low part of the Geldingadalir valley (Pedersen et al. 2022). This eruptive fissure was located right above the southern-middle part of the 9-km-long dike which had first been detected 19 days before, on a Sentinel interferogram spanning 23 February to 1 March 2021 (Sigmundsson et al. 2022). By the second day, the eruption had concentrated on two vents. These were the most active vents on the initial eruptive fissure which had been detected during the first night of the eruption (Figs. 2, 3, and 4).
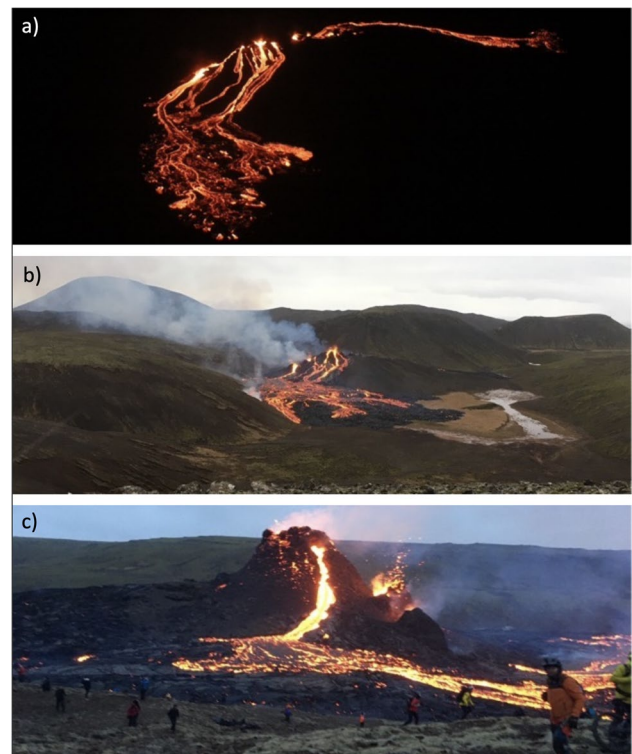

Fig. 3 The initial fissure opening. **a** Photo taken by Freysteinn Sigmundsson in the night from 19 to 20 March, about 4.5 h after the start of the eruption. **b** The morning after, about 11.5 h after the start of the eruption. **c** On the 21 March (19:47), the eruption had already mostly concentrated on two vents on the eruptive fissure, those vents are among the most active ones on the first photos (**a**, **b**)

The high-resolution ICEYE interferogram spanning one whole day, from 17 h before the eruption started until 7 h after it began (03:20 19 March to 03:20 20 March), showed different types of crustal deformation (Fig. 5). It showed the deformation due to a dikelet, which includes subsidence on and around the top of the dike, as well as the typical outward motion/extension pattern as a result of its emplacement. The image also showed small-scale fault movements on several faults which occurred during this period.

The second set of eruptive fissures opened on 5 April, about 1 km north-northeast of the original vents (Figs. 2 and 4). In this case, two eruptive fissures opened where the dike crossed pre-existing fractures, the latter of which could be seen on older aerial photographs and digital elevation models. The N-S orientation of the fractures suggest that they are most likely strike-slip faults (e.g., Einarsson et al. 2023). These eruptive fissures were closer to the center of the subsidence area, although slightly to the east of the center of the subsidence (Fig. 5). The fissures were approximately 85 and 20 m long and located on a topographically higher part than the first fissure. The third fissure opening occurred at midnight on 6–7 April and was about 100 m long. The fourth opening occurred on a ~90-m-long fissure. The last fissure openings occurred on 13 April. These fissures opened both to the north and south of the fissure that opened on the 6–7 April. The new fissures to the south were about 110 m long,

whereas the one to the north had a length of about 20 m. The southernmost and northernmost eruptive fissures were therefore the first ones to open, whereas the latter openings occurred between these two eruptive fissures. By the end of April, all vents had stopped erupting except the most southerly eruptive fissure that opened on 13 April. This eruptive fissure became dominant and the only active fissure until the end of the eruption on 18 September 2021.

The location of the eruptive vents with respect to pre-existing fractures and deformation during the first day of the eruption

The Fagradalsfjall area is cut by several north-south-oriented strike-slip faults and a few NE-oriented conjugate strike-slip faults. These faults can be observed from both aerial photographs and digital elevation models (Fig. 2), as well as by relocating earthquakes that have originated in the area since seismic measurements started (Hjaltadóttir and Vogfjörð 2006; Einarsson et al. 2023). In addition, a NNE-SSW striking hyaloclastite ridge, formed by subglacial eruption, is located just east of the 2021 eruption. During the unrest period in 2021 when the dike was propagating, multiple strike-slip earthquakes occurred, and surface ruptures were seen along several N-S-oriented strike-slip faults, where earthquakes larger than magnitude ~M5 had occurred.

Fig. 4 The evolution of new vent openings during the eruption in Fagradalsfjall. All frames show the same location, therefore showing how the eruption started in the southern part, the second opening occurred in the northern part and the later vent openings occurred in between. The aerial photographs are from the surveillance flights which were done repeatedly during the eruption (Pedersen et al. 2022); the imagery was processed at the Icelandic Institute of Natural History and the National Land Survey of Iceland. The aerial photographs behind the surveillance photograph on 20 March and a small part from 21 April is an aerial photograph from 2019 from Loftmyndir Corp
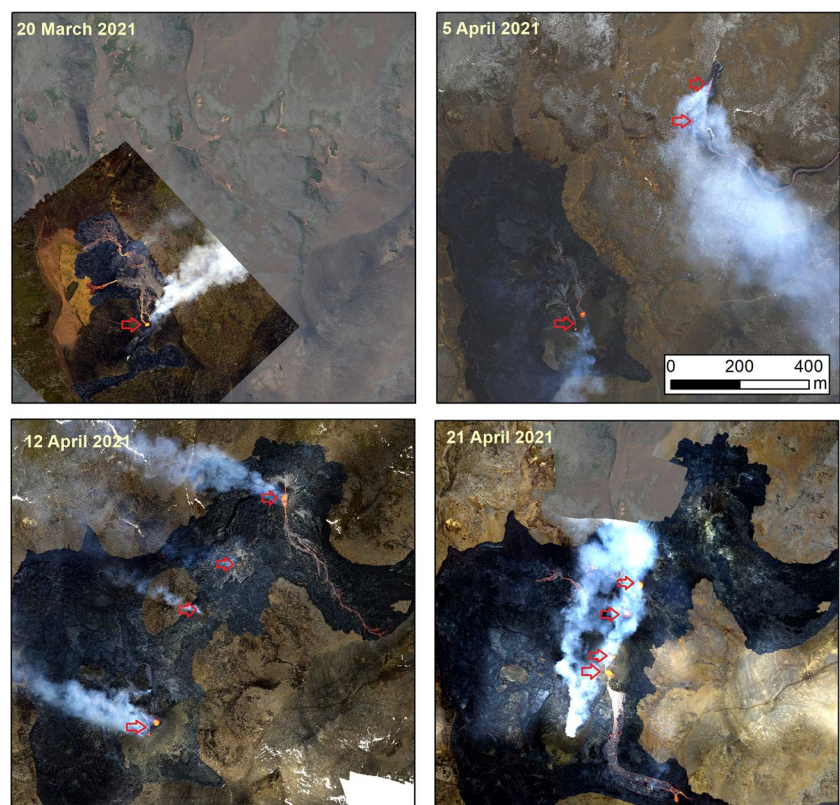
The 2021 eruptive fissure was generally oriented NNE-SSW, which is in accordance with the strike of the underlying dike, as determined from InSAR analysis, geodetic modeling, and seismicity (Sigmundsson et al. 2022). However, there are local deviations, which are located where the dike intersected the most prominent N-S strike slip faults. At these locations, the eruptive fissure bends slightly towards the N-S direction (Fig. 2).

The high-resolution ICEYE interferogram which spanned the first day of the eruption showed deformation on several north-south-oriented lineaments, which are most likely strike-slip faults (Fig. 5). The highest density of these strike-slip faults was northeast of the initial eruption site. In addition, new movements on a few NNE-oriented faults were detected, located east of the eruption site and the dike (Fig. 5). These faults were situated close to an inferred fault
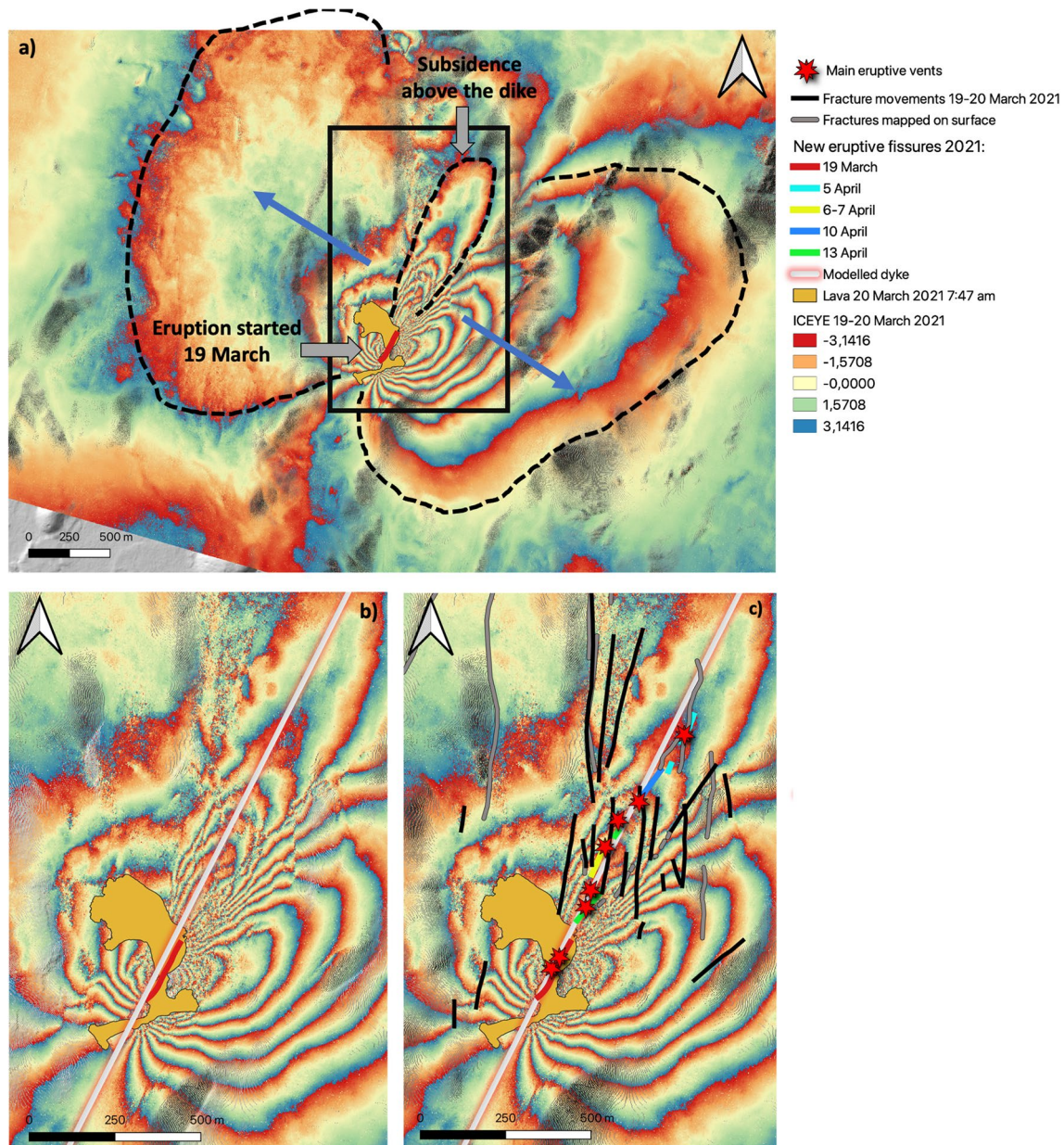
Fig. 5 Opening of new eruptive vents in April compared with where ICEYE interferograms showed deformation during and just before the first vent openings 19–20 March (red line). The ICEYE image shows the difference between the phase component of two radar images, taken at (03h:20m:56s) on 19 and 20 March 2021. (**a**) An overview of the ICEYE image, dotted lines delineate the typical butterfly shape of a dike intrusion with subsidence above the dike. Blue arrows show how the dike pushes the crust in opposite directions. (**b**) A close-up of the area where the eruptions occurred (black frame in panel **a**). The ICEYE image shows dislocations along N-S-oriented fractures, which are marked as black lines in panel **c**. There, gray lines show faults visible on DEMs and aerial photographs taken before the eruption. The new eruptive fissures and main vents are also shown

in the eastern part of the ICEYE interferogram. Some of the strike-slip faults that are seen on the ICEYE interferogram are visible on aerial photographs and DEMs from before the events, whereas others are not. Interestingly, most of the vent openings in April occurred at the intersection of the dike and these north-south-oriented strike-slip faults or a pre-existing strike-slip fault (Fig. 5). This observation is important in eruptions like those in Fagradalsfjall, where thousands of people came to see the eruption, and new hazard assessments were required on a regular basis.

Deformation modeling for 19 to 20 March 2021

Geodetic modeling was undertaken to determine the source parameters responsible for the main deformation observed in the 1-day ICEYE interferogram. A series of Bayesian inversions were run using a modified version of GBIS software (Bagnardi and Hooper 2018) and the ICEYE interferogram as the input. We intially ran this model just incorporating a single Okada dislocation (Okada 1985) to fit the deformation field; however, the misfit was significant and it was apparent

that a second deformation source was required. The best-fit dual source model comprised both opening on a dike and right-lateral strike-slip and dip-slip motion on a separate fault plane to the east of the dike, both modeled as Okada dislocations (Okada 1985). The dike was near-vertical, ~ 800 m long, extending from about 700-m depth to the surface, striking at 29 degrees with an opening of 22 cm. The fault had a length of ~ 1100 m, striking at 40 degrees (Figs. 6 and 7).

The opening process of the new eruptive fissures

During the eruption, several of the new eruptive fissure openings were monitored by webcams. These webcams show the time evolution from the start of steam rising from the fissure until a red glow, indicating eruption onset, can be seen. The time from the first observation of steam until the visual appearance of glowing lava ranged between 9 and 23 min during daytime and between 15 s and 1.5 min during night observation (Fig. 8). The difference in time can likely be explained by the different lighting conditions during day and night.

In all observed vent openings in April, there was visible steam emitted from the fissures that fed the various eruptions.
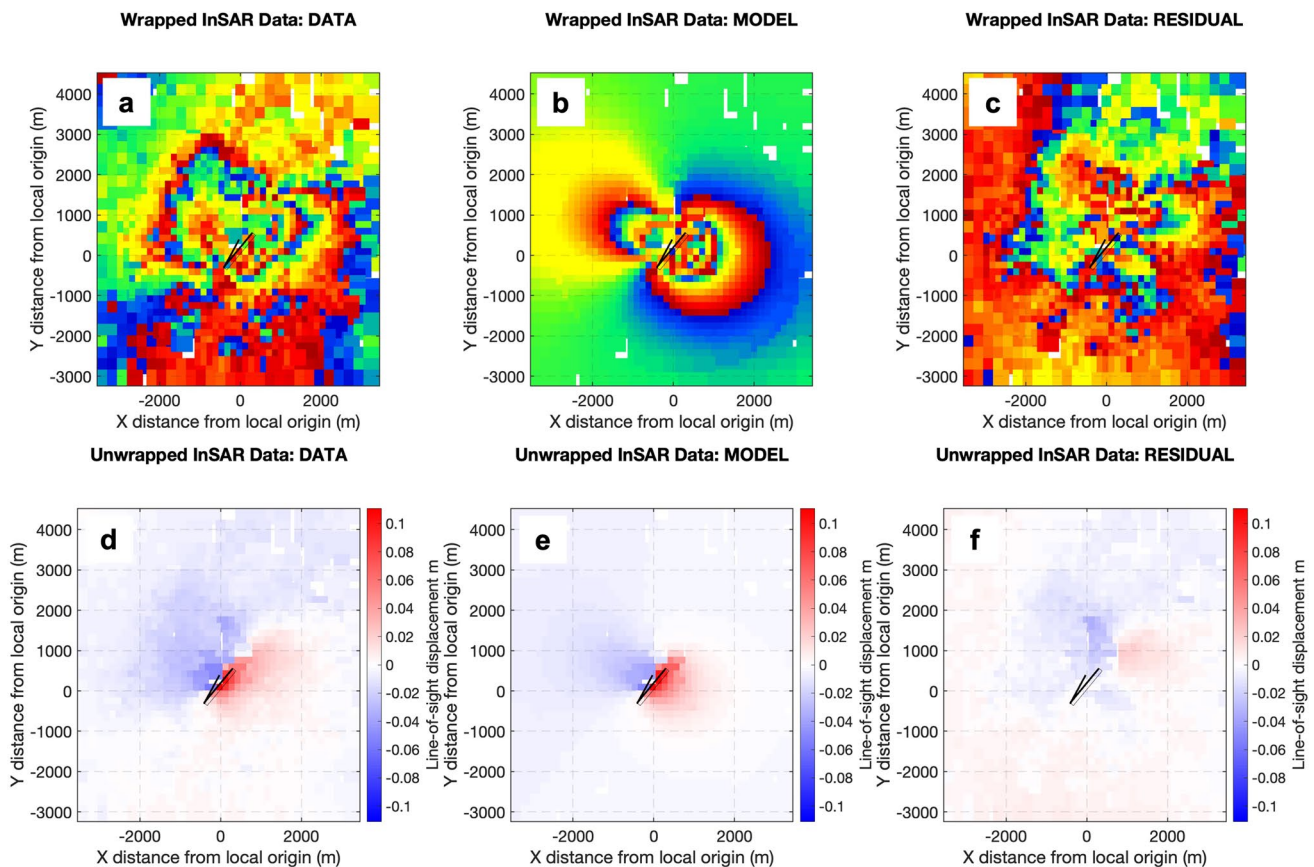

Fig. 6 Geodetic modeling results. **a**, **d** ICEYE interferogram from 19 to 20 of March 2021. **b**, **e** The best fit model includes both a dike (black line) and a fault (narrow black box to the east of the dike). **c**, **f** Residuals
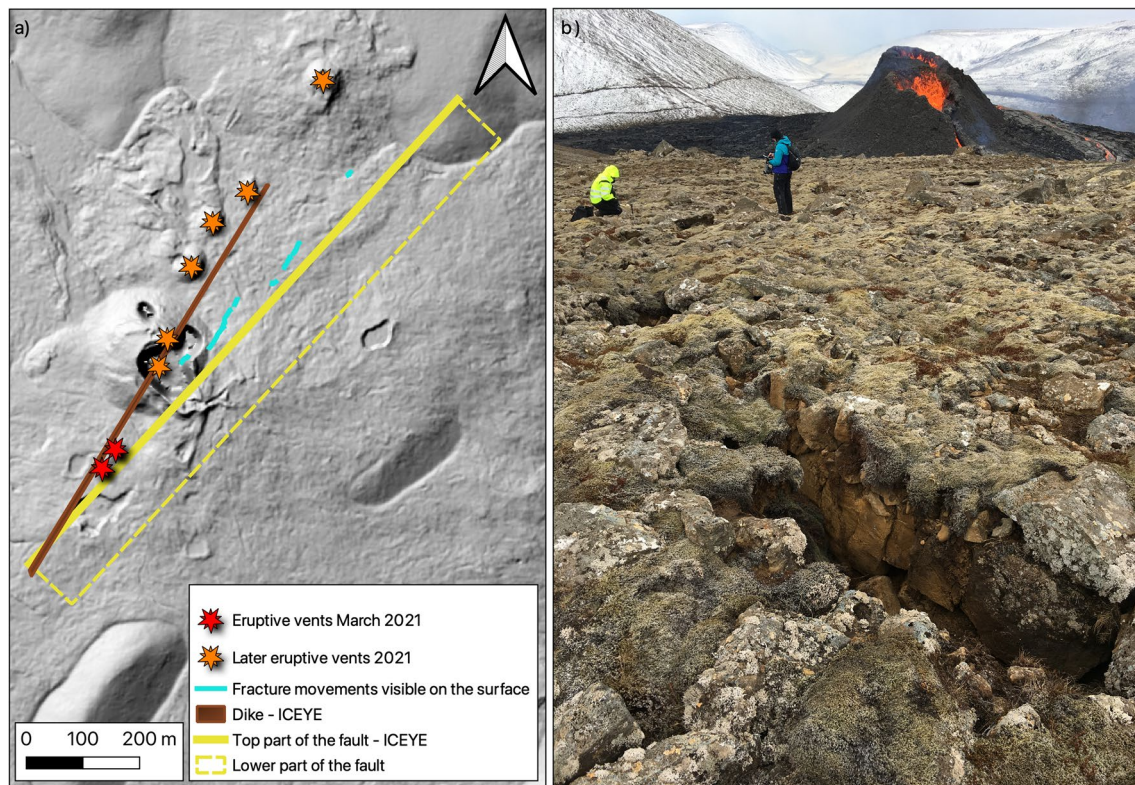
Fig. 7 **a** The results of the model in Fig. 6 plotted with the eruptive vents and new surface fracture movements, which were mapped in the field. Note how the surface of the modeled fault fits with the fracture movements seen on the surface. The ICEYE dike is the dikelet, i.e., a localized extension/conduit from the uppermost part of the 9-km-long dike. **b** An example of the new fault movements detected near the eruption (see blue lines in **a**). This fault was a part of the NNE-oriented fault system which delineated the eastern boundary of a shallow subsidence area detected on the ICEYE image from 19 to 20 March. The photo was taken on 25 March at 14:09. View towards the south

The steam emission increased until the first lava erupted. The opening of vent 2 (at 11:49 on 5. April), occurred only ~200 m from a mobile first-aid tent of one of the Icelandic Search and Rescue (SAR) teams. Despite the closeness of the vent, the SAR team was lucky that the topography of the area gave them enough time to dismantle the tent and evacuate within the next 2 h. From the footage showing the opening of vent 3 (midnight to 7 April), it can be observed that the eruption of lava was not accompanied by any violent fountaining. Instead, the initial lava production was effusive and similar to the upwelling surface of boiling porridge. While starting relatively gently, within only a minute, the first mild spattering occurred and the production of lava quickly escalated. Vents 5 and 6 opened beneath existing lava flows, and showed a very similar effusive behavior as for vent 3 (see also Fig. 2.2(A) in Gallagher (2021)).

Discussion
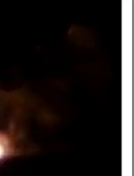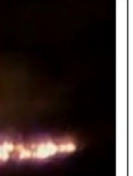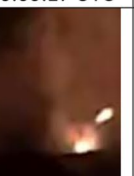
The relationship between fissure openings and pre-existing fractures during the eruption

Although there is not a prominent fissure swarm where the 2021 dike intrusion and eruption occurred, the strike-slip faults there are quite prominent. They had been detected before on aerial photographs and during fieldwork (e.g., Clifton and Kattenhorn 2006). NNE-oriented hyaloclastite ridges are also located in the area, formed by subglacial fissure eruption(s) during the Pleistocene (Sæmundsson et al. 2010). The strike-slip faults have been seismically active since precise seismic monitoring started in the 1970s (Klein et al. 1977; Einarsson 1991; Jakobsdóttir 2008; Keiding et al. 2009; Björnsson et al. 2020). Relative relocations of earthquakes which occurred between the years of 1997 and 2005 have depicted these strike-slip faults well, with the prominent N-S-oriented strike-slip faults, but also the conjugate ENE-oriented strike-slip faults (Hjaltadóttir and Vogfjörð 2006). These strike-slip faults can be considered

Fig. 8 **a** The opening of new eruptive vents, showing the development in time from the first observation of steam until the eruption starts. Note that the incandescence seen before on the figure for vent 4 is lava from another vent. The imagery is from time-lapse cameras and web cameras in the field, operated by the Institute of Earth Sciences at the University of Iceland, the Morgunblaðið newspaper and the Icelandic National Broadcasting Service (Ríkisútvarpið). No image from the opening of the first vent is available. **b** The time (in minutes) from the start of visible steam to the start of visible lava. The graph shows how the time difference is greater during daytime than during the night

a)

	before	first steam	more steam	first lava	evolved
vent 2 Initial fissure lengths: 20 and 85 m	05/04/2020 11:48:56 UTC	05/04/2020 11:49:56 UTC	05/04/2020 11:50:56 UTC	05/04/2020 12:12:56 UTC	05/04/2020 21:03:56 UTC
vent 3 Initial fissure length: 100 m	07/04/2021 00:00:01 UTC	07/04/2021 00:00:02 UTC	07/04/2021 00:00:11 UTC	07/04/2021 00:00:17 UTC	07/04/2021 00:03:33 UTC
vent 4 Initial fissure length: 90 m	10/04/2021 03:12:37 UTC	10/04/2021 03:13:01 UTC	10/04/2021 03:14:13 UTC	10/04/2021 03:14:37 UTC	10/04/2021 05:48:37 UTC
vent 5 Initial fissure length: 110 m	13/04/2021 08:27:16 UTC	13/04/2021 08:28:16 UTC	13/04/2021 08:33:16 UTC	13/04/2021 08:37:16 UTC	13/04/2021 19:15:16 UTC
vent 6 Initial fissure length: 20 m	13/04/2021 08:34:16 UTC	13/04/2021 08:35:16 UTC	13/04/2021 08:39:16 UTC	13/04/2021 08:44:16 UTC	13/04/2021 19:15:16 UTC

b)
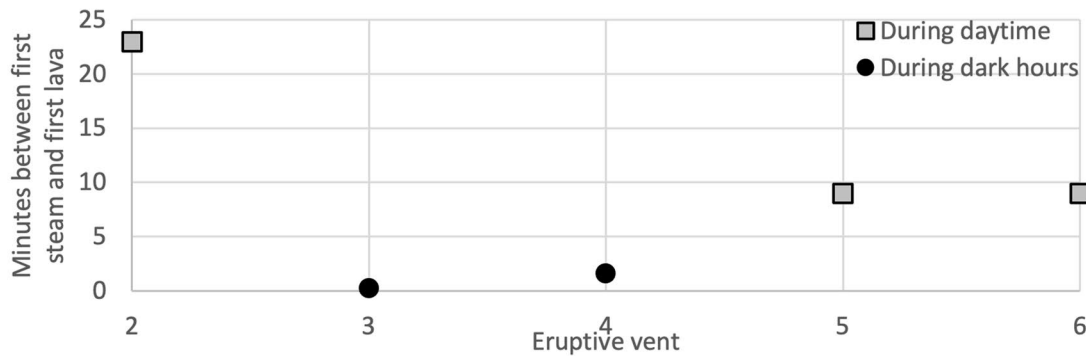
to be zones of structural weakness above and around the NNE-oriented propagating dike in February and March 2021, and therefore potential magma migration pathways and locations of eventual eruptive vents. It is nevertheless noteworthy that the eruptive vents mostly occurred along the prominent N-S-oriented strike-slip faults, not along the less-prominent ENE-oriented strike-slip faults.

The deformation detected along some of these strike-slip faults in the ICEYE interferogram spanning the first day of the eruption may also have been used to forecast the location of potential openings along these lineaments. The interaction between the dike and the pre-existing strike-slip faults can thus serve as a guide for implementing exclusion zones during future fissure eruptions in the southern to middle part of the Reykjanes peninsula, i.e., along the zone of strike-slip faults.

Subsidence near the eruptive fissures

A visible graben was not formed above the dike, although a subsidence signal was detected above the dike on the ICEYE image and fractures were mapped in the field which followed the NNE-oriented direction of this subsidence (Fig. 5). These fractures were located to the east of the dike and the eruptive fissures. They were closest to the eruptive fissure which opened on 13 April (~30 m), but farther away from the northern eruptive fissures (~130 m). A lineament is also observed in the interferogram where the new fracture movements were detected in the field. This corresponds to the fault that was required in the geodetic model (in addition to the dike) to fit the deformation field observed in the ICEYE interferogram. However, the modeled fault is dipping towards the SE, which thus is not interpreted to be a graben fault which would have an inward dip towards the dike, i.e., more towards the NW. The indications of a narrow subsidence in the southern part suggest the dike was very close to the surface there. This area is where the most active vent of the entire eruption was located.

The question thus arises: what controls whether or not grabens form above dikes? Previous studies have indicated that graben formation depends on various factors, such as the layer properties of the strata in which the dike propagates, the pressure of the magma in the dike, the top-depth of the dike, and the regional stress field (e.g., Pollard et al. 1983; Al Shehri and Gudmundsson 2018; Bazargan and Gudmundsson 2019). Additional studies are required at Fagradalsfjall to determine why a graben did not form above the February–March 2021 dike (or the July-August 2022 dike).

A comparison with other eruptive fissures in the Reykjanes peninsula

The question arises as to whether the interaction of dike intrusions with strike-slip faults is common for fissure eruptions in the Reykjanes peninsula. A comparison with other eruptive fissures in the southern to middle part of the Reykjanes peninsula shows that some of the eruptive fissures are very oblique and far from being perpendicular to the plate spreading vector, as would be expected if they were formed in a pure extensional setting (Fig. 9) (Eyjólfsson 1998). The eruptive fissures or parts of them also often follow the en-echelon pattern which is typical of strike-slip faults (Jenness and Clifton 2009; Einarsson et al. 2020). In addition, some glaciovolcanic edifices follow the orientation of strike-slip faults (Pedersen and Grosse 2014). Nevertheless, many of the eruptive fissures do have the northeasterly orientation that is perpendicular to the plate spreading direction in the area. The other eruptive segments are oriented north-south or towards the east-northeast, i.e., in the same direction as the strike-slip faults in the area (Fig. 9). This suggests that those eruptive fissures were formed by magma penetrating through the pre-existing strike-slip faults. The strike-slip faults are only found in a central zone extending in an east-west direction through the southern to middle part of the peninsula, whereas normal faults exist farther towards the north. The general trend of the fissure swarms in Reykjanes tends to bend more towards the ENE direction in the northern part. There, the eruptive fissures are mostly parallel with the fractures in the fissure swarms and thus likely did not interact with strike-slip features.

Compared to other parts of the plate boundary in Iceland where oblique spreading is not taking place, these eruptive fissures are generally not as linear as the eruptive fissures at the pure extensional fissure swarms. This feature likely stems from the oblique spreading of the Reykjanes peninsula and the interaction with the strike-slip faults.

Why do eruptions through strike-slip faults occur?

Other examples of eruptions through strike-slip faults are known, both in Iceland and from other tectonic settings, such as in Argentina (Spacapan et al. 2016), in Antarctica (Rossetti et al. 2000), Turkey (Adiyaman et al. 1998), and in West Iceland (Khodayar and Einarsson 2002).

There have been different suggestions as to how these eruptions occur. The eruptions can occur on the pull-apart basins part of the fault, at the horse tail structure, on the releasing bend of the strike-slip fault, or on a pure strike-slip fault (Tibaldi et al. 2009). In the case of Fagradalsfjall, the eruptive vents seem to be located on the parts of the faults which are pure strike-slip faults, since we do not see any evidence of other features such as pull-apart basins where the vents are located.

The question also arises why the magma erupts through and concentrates at vents within the strike-slip faults, i.e.,

why the existing strike-slip faults were used as feeder dikes. It is likely that the magma is migrating through existing zones of weakness in the crust, although in this instance the exact conditions as to why these propagation paths were favorable are unknown. However, previous studies have indicated that whether or not a dike propagates through an existing fault can depend on different factors, for example the fault's tensile strength when compared with the tensile strength of the surrounding rock, the fault's dip, and the

normal stress applied to the fault (compared with the minimum principal compressive stress) (Gudmundsson 2022). It is also noteworthy that the magma influx rate to the dike was quite low (<10 m^3/s) during its final ascent to the surface (Sigmundsson et al. 2022; Einarsson et al. 2023), which was consistent with the low lava effusion rates which were measured at the eruption onset (Pedersen et al. 2022). This may have caused the pre-existing fractures to play a larger role in facilitating magma migration to the surface. If

Fig. 9 A comparison of the location and style of the eruptive fissures at the Fagradalsfjall eruption (seen in panel **a**) with other eruptive fissures in the vicinity of the eruption. Red lines denote eruptive fisures and the purple dotted lines in panel **a** show the main strike-slip faults there. (**b**) The ~2000-year-old eruptive fissure of the Skollahraun lava. (**c**) The 1151–1188 AD eruptive fissure of the Ögmundarhraun lava. The red eruptive fissures in panels **c** and **d** were mapped by Clifton and Kattenhorn (2006)
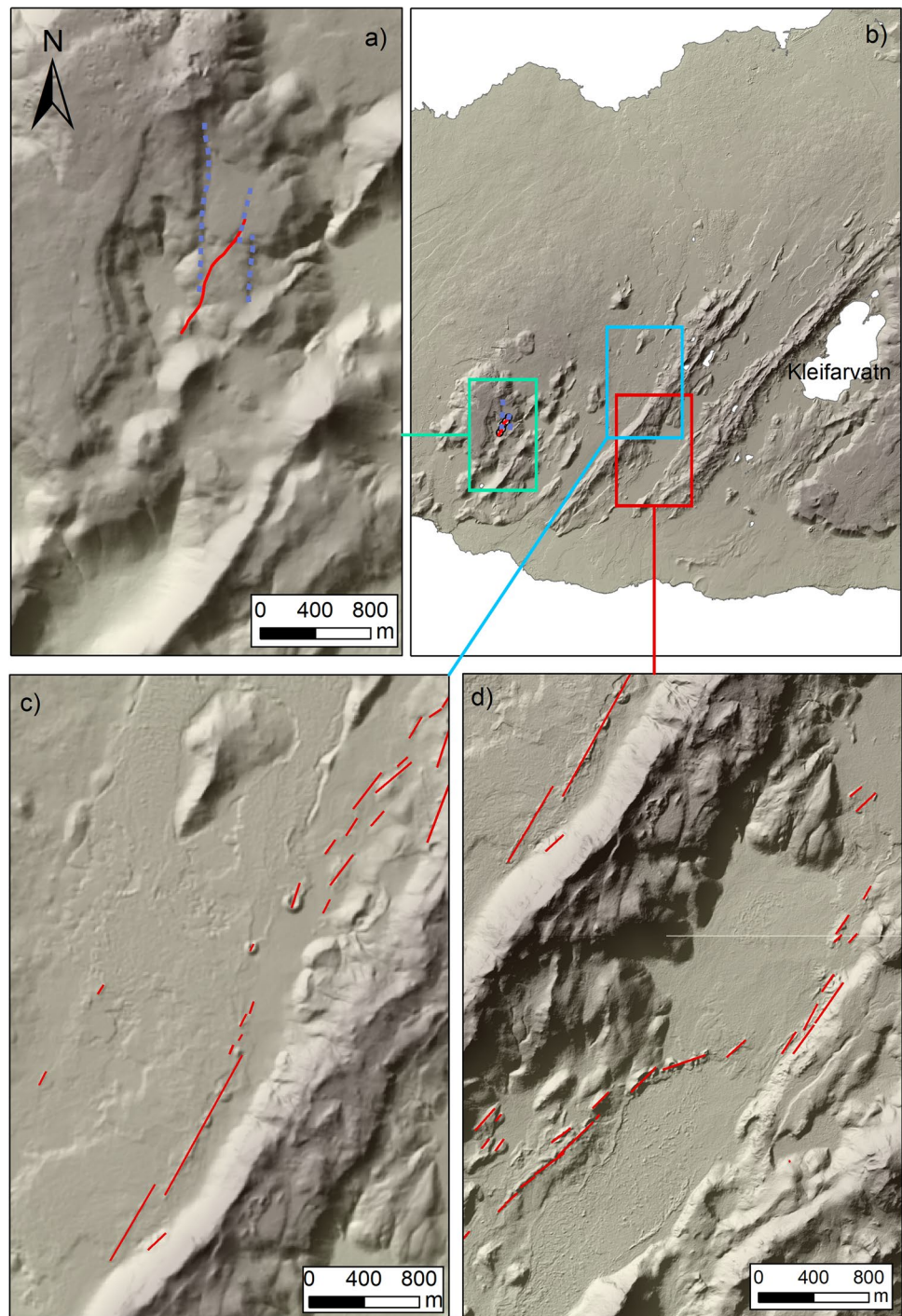
the overpressure in the dike had been significantly higher, magma migration may have been less influenced by pre-existing fractures in the area. However, in this case, we suggest the faults were zones of structural weakness in the crust, therefore pathways of least resistance for magma to propagate through.

Conclusions

The 2021 Fagradalsfjall eruption offered a unique opportunity to study how eruptive fissures open in oblique rifts. This eruption demonstrated how pre-existing strike-slip faults may act as a pathway for magma to migrate through from an underlying dike and thus how previous detailed mapping of faults in the area can be used for risk assessment, both before the eruption but also for hazard and risk assessment during the eruption, to forecast where new vent openings could occur.

Detailed monitoring of deformation in the area, such as the use of high resolution ICEYE interferograms, can be used to show which of the faults moved during unrest and are thus candidates for future vent locations. The 1-day interferogram from ICEYE incorporated in this study, spanning the first day of the eruption from 19 to 20 March, showed detailed deformation along the strike-slip faults that became the locations of the several vent openings occurring in April.

Lava eruptions in easily accessible areas, such as the Reykjanes peninsula, can become very popular attractions for the public, as was the case for the 2021 Fagradalsfjall eruption, where 356 thousand visitors were recorded (Barsotti et al. 2022). It is therefore extremely important to understand how and where new eruptive vents may open: does it happen so quickly that people cannot evacuate, or does it take time? By using time-lapse cameras and webcams, we show that for the Fagradalsfjall eruption, during daytime, it took only 9 to 23 min for a new vent to open, starting from a new source of steam until a red glow was visible. It is questionable if such a short warning period would necessarily be sufficient to evacuate bystanders from the vent-forming area. Furthermore, it should be stressed that the visibility conditions are a crucial factor when it comes to hazard response with regard to the opening of a new vent. While it is easy to detect the emission of steam in broad daylight, the warning time for an imminent opening of a new vent is, according to our findings on Fagradalsfjall, drastically reduced—from minutes to only seconds—during night time.

This study highlights the importance of utilizing interferograms of high temporal and spatial resolution during future diking events. We expect the ongoing unrest of the Reykjanes Peninsula oblique rift to provide further opportunities to study how small-scale fracture movements relate to future eruptive vent openings. This is of crucial importance on the Reykjanes peninsula, where dike intrusions may occur close to, or even within, inhabited areas.

Declarations

Competing interests The authors declare no competing interests.

References

Abdallah A, Courtillot V, Kasser M, Ledain AY, Lepine JC, Robineau B, Ruegg JC, Tapponnier P, Tarantola A (1979) Relevance of Afar seismicity and volcanism to the mechanics of accreting plate boundaries. Nature 282(5734):17–23

Adiyaman Ö, Chorowicz J, Köse O (1998) Relationships between volcanic patterns and neotectonics in Eastern Anatolia from analysis of satellite images and DEM. J Volcanol Geotherm Res 85(1-4):17–32

Al Shehri A, Gudmundsson A (2018) Modelling of surface stresses and fracturing during dyke emplacement: application to the 2009 episode at Harrat Lunayyir, Saudi Arabia. J Volcanol Geotherm Res 356:278–303

Árnadóttir T, Lund B, Jiang W, Geirsson H, Björnsson H, Einarsson P, Sigurðsson T (2009) Glacial rebound and plate spreading: results from the first countrywide GPS observations in Iceland. Geophys J Int 177(2):691–716

Bagnardi M, Hooper A (2018) Inversion of surface deformation data for rapid estimates of source parameters and uncertainties: a Bayesian approach. Geochemistry, Geophys Geosystems 19(7):2194–2211

Barsotti S, Parks MM, Pfeffer MA, Óladóttir BA, Barnie T, Titos MM, Jónsdóttir K, Pedersen G, Hjartardóttir ÁR, Stefansdóttir G, Jóhannsson T, Arason Þ, Gudmundsson MT, Oddsson B, Þrastarson RH, Ófeigsson BG, Vogfjörd K, Geirsson H, Hjörvar T, von Löwis S, Petersen GN, Sigurðsson EM (2023) The eruption in Fagradalsfjall (2021, Iceland): how the operational monitoring and the volcanic hazard assessment contributed to its safe access. Nat Hazards 116:3063–3092

Bazargan M, Gudmundsson A (2019) Dike-induced stresses and displacements in layered volcanic zones. J Volcanol Geotherm Res 384:189–205

Biggs J, Amelung F, Gourmelen N, Dixon TH, Kim SW (2009) InSAR observations of 2007 Tanzania rifting episode reveal mixed fault and dyke extension in an immature continental rift. Geophys J Int 179(1):549–558

Björnsson A, Sæmundsson K, Einarsson P, Tryggvason E, Grönvold K (1977) Current rifting episode in North Iceland. Nature 266:318–323

Björnsson S, Einarsson P, Tulinius H, Hjartardóttir ÁR (2020) Seismicity of the Reykjanes Peninsula 1971–1976. J Volcanol Geotherm Res 391:106369

Bruce PM, Huppert HE (1990) Solidification and melting along dykes by the laminar flow of basaltic magma. In: Ryan MP (ed) Magma transport and storage (chapter 6). John Wiley & Sons Ltd, pp 87–101

Clifton AE, Kattenhorn SA (2006) Structural architecture of a highly oblique divergent plate boundary segment. Tectonophysics 419(1-4):27–40

DeMets C, Gordon RG, Argus DF, Stein S (1994) Effect of recent revisions to the geomagnetic reversal time-scale on estimates of current plate motions. Geophys Res Lett 21(20):2191–2194

Einarsson P (1991) Earthquakes and present-day tectonism in Iceland. Tectonophysics 189(1-4):261–279

Einarsson P (2008) Plate boundaries, rifts and transforms in Iceland. Jökull 58:35–58

Einarsson P, Brandsdóttir B (2021) Seismicity of the Northern Volcanic Zone of Iceland. Front Earth Sci 9:166

Einarsson P, Eyjólfsson V, Hjartardóttir ÁR (2023) Tectonic framework and fault structures in the Fagradalsfjall segment of the Reykjanes Peninsula Oblique Rift, Iceland. Bull Volcanol 85(2):9

Einarsson P, Hjartardóttir ÁR, Imsland P, Hreinsdóttir S (2020) The structure of seismogenic strike-slip faults in the eastern part of the Reykjanes Peninsula oblique rift. SW Iceland. J Volcanol Geotherm Res 391:106372

Einarsson P, Sæmundsson K (1987) Earthquake epicenters 1982-1985 and volcanic systems in Iceland (map). In: Sigfússon ÞI (ed) Í hlutarins eðli, Festschrift for Þorbjörn Sigurgeirsson. Menningarsjóður, Reykjavík

Eyjólfsson V (1998) Mapping of fractures and Holocene volcanic fissures at Fagradalsfjall in the western Reykjanes Peninsula (B.Sc. thesis, in Icelandic). In: Faculty of Earth Sciences. University of Iceland, Reykjavík, Iceland, p 70

Gallagher CR (2021) The timing and mechanisms of sulfur release by Icelandic flood lava eruptions:Holuhraun 2014–15 CE and Laki 1783–84 CE a case study. In: Faculty of Earth Sciences. University of Iceland, Reykjavík

Geirsson H, Parks M, Vogfjörd K, Einarsson P, Sigmundsson F, Jónsdóttir K, Drouin V, Ófeigsson BG, Hreinsdóttir S, Ducrocq C (2021) The 2020 volcano-tectonic unrest at Reykjanes Peninsula, Iceland: stress triggering and reactivation of several volcanic systems. EGU General Assembly Conference Abstracts: EGU21–E7534

Gudmundsson A (2020) Volcanotectonics: understanding the structure, deformation and dynamics of volcanoes. Cambridge University Press, p 598

Gudmundsson A (2022) The propagation paths of fluid-driven fractures in layered and faulted rocks. Geological Magazine, pp 1–24

Guðmundsson Á (1987) Geometry, formation and development of tectonic fractures on the Reykjanes peninsula, southwest Iceland. Tectonophysics 139(3-4):295–308

Halldórsson SA, Marshall EW, Caracciolo A, Matthews S, Bali E, Rasmussen MB, Ranta E, Robin JG, Guðfinnsson GH, Sigmarsson O, Maclennan J, Jackson MG, Whitehouse MJ, Jeon H, van der Meer QHA, Mibei GK, Kalliokoski MH, Repczynska MM, Rúnarsdóttir RH, Sigurðsson G, Pfeffer MA, Scott SW, Kjartansdóttir R, Kleine BI, Oppenheimer C, Aiuppa A, Ilyinskaya E, Bitetto M, Giudice G, Stefánsson A (2022) Rapid shifting of a deep magmatic source at Fagradalsfjall volcano, Iceland. Nature 609:529–534

Hjaltadóttir S, Vogfjörð KS (2006) Kortlagning sprungna í Fagradalsfjalli á Reykjanesskaga með smáskjálftum. Technical report, Iceland Meteorological Office, 2006a. Report VÍ-ES-01

Hjartardóttir ÁR, Einarsson P, Gudmundsson MT, Högnadóttir T (2016) Fracture movements and graben subsidence during the 2014 Bárðarbunga dike intrusion in Iceland. J Volcanol Geotherm Res 310:242–252

Hreinsdóttir S, Einarsson P, Sigmundsson F (2001) Crustal deformation at the oblique spreading Reykjanes Peninsula, SW Iceland: GPS measurements from 1993 to 1998. Journal of Geophysical Research: Solid Earth 106(B7):13803–13816

Jakobsdóttir SS (2008) Seismicity in Iceland: 1994-2007. Jökull 58:75–100

Jenness MH, Clifton AE (2009) Controls on the geometry of a Holocene crater row: a field study from southwest Iceland. Bull Volcanol 71(7):715–728

Jónsson J (1978) Geological map of the Reykjanes Peninsula. Orkustofnun, report OS-JHD 7831:332

Keiding M, Lund B, Árnadóttir T (2009) Earthquakes, stress, and strain along an obliquely divergent plate boundary: Reykjanes Peninsula, Southwest Iceland. J Geophys Res Solid Earth 114:B09306

Khodayar M, Einarsson P (2002) Strike-slip faulting, normal faulting, and lateral dike injections along a single fault: field example of the Gljúfurá fault near a Tertiary oblique rift-transform zone, Borgarfjörður, west Iceland. J Geophys Res 107(B5):ETG 5-1-ETG 5-16

Klein FW, Einarsson P, Wyss M (1977) Reykjanes peninsula, Iceland, earthquake swarm of september 1972 and its tectonic significance. J Geophys Res 82(5):865–888

Nakamura K (1977) Volcanoes as possible indicators of tectonic stress orientation — principle and proposal. J Volcanol Geotherm Res 2(1):1–16

Neal CA, Brantley S, Antolik L, Babb J, Burgess M, Calles K, Cappos M, Chang J, Conway S, Desmither L (2019) The 2018 rift eruption and summit collapse of Kīlauea Volcano. Science 363(6425):367–374

Okada Y (1985) Surface deformation due to shear and tensile faults in a half-space. Bull Seismol Soc Am 75(4):1135–1154

Pedersen G, Grosse P (2014) Morphometry of subaerial shield volcanoes and glaciovolcanoes from Reykjanes Peninsula, Iceland: effects of eruption environment. J Volcanol Geotherm Res 282:115–133

Pedersen GB, Belart JM, Óskarsson BV, Gudmundsson MT, Gies N, Högnadóttir T, Hjartardóttir ÁR, Pinel V, Berthier E, Dürig T, Reynolds HI, Hamilton CW, Valsson G, Einarsson P, Ben-Yehosua D, Gunnarsson A, Oddsson B (2022) Volume, effusion rate, and lava transport during the 2021 Fagradalsfjall eruption: results from near real-time photogrammetric monitoring. Geophys Res Lett 49(13):e2021GL097125

Pollard DD, Delaney PT, Duffield WA, Endo ET, Okamura AT (1983) Surface deformation in volcanic rift zones. Tectonophysics 94(1):541–584

Porter C, Morin P, Howat I, Noh MJ, Bates B, Peterman K, Keesey S, Schlenk M, Gardiner J, Tomko, K, Willis M, Kelleher C, Cloutier M, Husby E, Foga S, Nakamura H, Platson M, Wethington MJ, Williamson C, Bauer G, Enos J, Arnold G, Kramer W, Becker P, Doshi A, D'Souza C, Cummens P, Laurier F, Bojesen M (2018) ArcticDEM, V1. https://doi.org/10.7910/DVN/OHHUK

Rossetti F, Storti F, Salvini F (2000) Cenozoic noncoaxial transtension along the western shoulder of the Ross Sea, Antarctica, and the emplacement of McMurdo dyke arrays. Terr Nova 12(2):60–66

Ruch J, Wang T, Xu W, Hensch M, Jónsson S (2016) Oblique rift opening revealed by reoccurring magma injection in central Iceland. Nature Comm 7:12352

Sæmundsson K (1978) Fissure swarms and central volcanoes of the neovolcanic zones of Iceland. In: Bowes DR, Leake BE (eds) Crustal evolution in northwestern Britain and adjacent regions. Seel House Press, Liverpool, England, pp 415–432

Sæmundsson K, Jóhannesson H, Hjartarson Á, Kristinsson SG, Sigurgeirsson MÁ (2010) Geological map of Southwest Iceland. Iceland Geosurvey

Sæmundsson K, Sigurgeirsson MÁ (2013) Reykjanesskagi. In: Sólnes J, Sigmundsson F, Bessason B (eds) Náttúruvá. Viðlagatrygging Íslands / Háskólaútgáfan, Reykjavík, pp 379–401

Sæmundsson K, Sigurgeirsson MÁ, Friðleifsson GÓ (2020) Geology and structure of the Reykjanes volcanic system. Iceland. J Volcanol Geotherm Res 391:106501

Sella GF, Dixon TH, Mao AL (2002) REVEL: a model for recent plate velocities from space geodesy. J Geophys Res-Solid Earth 107(B4):2081

Sigmundsson F, Hooper A, Hreinsdottir S, Vogfjord KS, Ofeigsson BG, Heimisson ER, Dumont S, Parks M, Spaans K, Gudmundsson GB, Drouin V, Arnadottir T, Jonsdottir K, Gudmundsson MT, Hognadottir T, Fridriksdottir HM, Hensch M, Einarsson P, Magnusson E, Samsonov S, Brandsdóttir B, White RS, Ágústsdóttir Th, Greenfield T, Green RG, Hjartardóttir ÁR, Pedersen R, Bennett RA, Geirsson H, La Femina PC, Björnsson H, Pálsson F, Sturkell E, Bean CJ, Möllhoff M, Braiden AK, Eibl EPS (2015) Segmented lateral dyke growth in a rifting event at Bardarbunga volcanic system, Iceland. Nature 517(7533):191–195

Sigmundsson F, Parks M, Hooper A, Geirsson H, Vogfjörd KS, Drouin V, Ófeigsson BG, Hreinsdóttir S, Hjaltadóttir S, Jónsdóttir K (2022) Deformation and seismicity decline before the 2021 Fagradalsfjall eruption. Nature 609:23–528

Sigurdsson O (1980) Surface deformation of the Krafla fissure swarm in two rifting events. J Geophys-Zeitschrift Fur Geophysik 47(1-3):154–159

Spacapan JB, Galland O, Leanza HA, Planke S (2016) Control of strike-slip fault on dyke emplacement and morphology. J Geol Soc 173(4):573–576

The National Land Survey of Iceland, ÍslandsDEM, V1 (2020). https://gatt.lmi.is/geonetwork/srv/metadata/e6712430-a63c-4ae5-9158-c89d16da6361

Tibaldi A, Pasquarè F, Tormey D (2009) Volcanism in reverse and strike-slip fault settings. In: New frontiers in integrated solid earth sciences. Springer, pp 315–348

Trippanera D, Acocella V, Ruch J, Abebe B (2015) Fault and graben growth along active magmatic divergent plate boundaries in Iceland and Ethiopia. Tectonics 34(11):2318–2348

Villemin T, Bergerat F (2013) From surface fault traces to a fault growth model: the Vogar Fissure Swarm of the Reykjanes Peninsula, Southwest Iceland. J Struct Geol 51(0):38–51

Wright TJ, Ebinger C, Biggs J, Ayele A, Yirgu G, Keir D, Stork A (2006) Magma-maintained rift segmentation at continental rupture in the 2005 Afar dyking episode. Nature 442(7100):291–294

Wright TJ, Sigmundsson F, Ayele A, Belachew M, Brandsdóttir B, Calais E, Ebinger C, Einarsson P, Hamling I, Keir D, Lewi E, Pagli C, Pedersen R (2012) Geophysical constraints on the dynamics of spreading centres from rifting episodes on land. Nat Geosci 5:242–250